Time reversal in attenuating acoustic media

Habib Ammari, Elie Bretin, Josselin Garnier, and Abdul Wahab

Abstract. In this paper we consider the problem of reconstructing sources in attenuating acoustic media using a time-reversal technique. We first justify the use of the adjoint of the attenuated wave operator instead of the ideal one for modifying the time-reversal process as a first order correction of the attenuation effect. Then we present a modified approach for higher order corrections. We use a thermo-viscous law model for the attenuation losses.

1. Introduction

Many inverse problems in biomedical imaging are concerned with the determination of strength and location of sources causing perturbations in the medium [**1, 3, 4, 6, 17**]. Given the measurements on a detection surface, these problems are equivalent to find the "initial conditions" on the wavefield. The goal of finding such initial conditions, can be achieved by using the so-called "time reversibility" of the wave equations in a non-dissipative medium. It is possible to reverse a wave from a "final state" in such a way that it retraces its original path back through the medium and refocusses on the source location. This provides the basis of the time-reversal technique. See for instance [**15, 16, 21, 14, 10, 11, 1, 17, 12**] and references therein for comprehensive details. See also [**8, 7, 23**] for applications of time reversal techniques in biomedical imaging.

In acoustic imaging, a challenging problem is to model the attenuation and to compensate its effect in image reconstruction [**5, 19**]. In this paper, we consider the problem of reconstructing sources in attenuating acoustic media using a time-reversal technique. It is motivated by the recent works on hybrid imaging using acoustics such as photoacoustic imaging [**3, 4, 2**], magneto-acoustic imaging [**6**], and radiation force imaging [**7**]; see also [**1**] and [**9**]. Classical time-reversal methods, without taking account of the attenuation effect, produce blurring in reconstructing source terms. Indeed attenuation is a key issue as it breaks the time reversibility of the wave equation. Some recent works propose to modify the time-reversal process, using the adjoint of the attenuated wave operator instead of the ideal one [**22, 13**]. In this paper, we aim to justify this technique as a first order correction of the attenuation effect. At the same time, we also present a modified approach for higher order corrections. We use a thermo-viscous law model for the attenuation losses. However, our

2010 *Mathematics Subject Classification.* Primary 35L05, 35R30; Secondary 47A52, 65J20.
Key words and phrases. Time reversal, wave propagation, attenuation.

analysis can be extended to more generalized power law attenuation models with fractional exponents.

The rest of the paper is organized as follows. In Section 2, we recall two classical time reversal methods for the acoustic wave equation in an ideal acoustic medium. In Section 3, we propose and analyze a time reversal method for attenuating acoustic media. In Section 4, we present an alternative approach which consists of preprocessing the data before applying classical time reversal algorithm. In Section 5, we present some numerical illustrations to compare different variants of the time reversal and to highlight the potential of our approach. Finally, the paper ends with a short discussion and a conclusion.

2. Time Reversal in Homogeneous Acoustic Media Without Attenuation

Let Ω be a smooth bounded domain in $\mathbb{R}^d$, $d = 2$ or 3. Consider the acoustic wave equation

$$\begin{cases} \dfrac{\partial^2 p}{\partial t^2}(x,t) - \Delta p(x,t) = \dfrac{d\delta_0}{dt}(t) f(x), \quad (x,t) \in \mathbb{R}^d \times [0,\infty[, \\ \\ p(x,t) = 0 \quad \text{and} \quad \dfrac{\partial p(x,t)}{\partial t} = 0, \qquad t \ll 0, \end{cases} \tag{2.1}$$

where δ_0 is the Dirac mass at $t = 0$ and the source f is smooth and has a smooth support $K \subset\subset \Omega$. We assume that f is a real-valued function. Equation (2.1) models photoacoustic imaging with f being the absorbed optical energy density [**3**].

Let $g(y,t)$ be defined as $g(y,t) := p(y,t)$ for all $y \in \partial\Omega$ and $t \in [0,T]$, where T is supposed to be sufficiently large such that $p(x,t) = 0 = \dfrac{\partial p(x,t)}{\partial t}$ for $t \geq T$ and $x \in \Omega$. It is easy to see that g is smooth. Our aim in this section is to reconstruct an approximation of the source f from g on $\partial\Omega \times [0,T]$.

We need the following notation. Let $\mathcal{F}$ denote the Fourier transform

$$\mathcal{F}[v](x,\omega) = \int_{\mathbb{R}} v(x,t) \exp(i\omega t) dt.$$

We also introduce

$$\Gamma(x,y,\tau,t) = \mathcal{F}^{-1}[\Gamma_\omega(x,y)](t-\tau) = \frac{1}{2\pi} \int_{\mathbb{R}} \Gamma_\omega(x,y) \exp(-i\omega(t-\tau)) d\omega,$$

where Γ_ω is the outgoing fundamental solution to the Helmholtz equation $-(\Delta + \omega^2)$ in $\mathbb{R}^d$:

$$(\Delta + \omega^2)\Gamma_\omega(x,y) = -\delta_x \quad \text{in } \mathbb{R}^d,$$

subject to the outgoing radiation condition.

2.1. Ideal Time Reversal Imaging Technique.

Introduce the solution v of the following wave problem

$$\begin{cases} \dfrac{\partial^2 v}{\partial t^2}(x,t) - \Delta v(x,t) = 0, \quad (x,t) \in \Omega \times [0,T], \\ v(x,0) = \dfrac{\partial v}{\partial t}(x,0) = 0, \qquad x \in \Omega, \\ v(x,t) = g(x, T-t) \qquad (x,t) \in \partial\Omega \times [0,T]. \end{cases}$$

The time-reversal imaging functional $\mathcal{I}_1(x)$ reads

$$\mathcal{I}_1(x) = v(x,T), \quad x \in \Omega.$$

In order to explicit $\mathcal{I}_1(x)$, introduce the Dirichlet Green function $G(x,y,\tau,t)$ defined as the solution of the following wave equation

$$\begin{cases} \dfrac{\partial^2 G}{\partial t^2}(x,y,\tau,t) - \Delta_y G(x,y,\tau,t) = \delta_x \delta_\tau, \quad (y,t) \in \Omega \times \mathbb{R}, \\ G(x,y,\tau,t) = 0, \quad \dfrac{\partial G}{\partial t}(x,y,\tau,t) = 0, \quad t \ll \tau, \\ G(x,y,\tau,t) = 0, \quad (y,t) \in \partial\Omega \times \mathbb{R}, \end{cases}$$

where δ_x and δ_τ are the Dirac masses at x and at τ.

Using the reversibility of the wave equation, we arrive at

$$\mathcal{I}_1(x) = v(x,T) = \int_0^T \int_{\partial\Omega} \frac{\partial G(x,y,T,t)}{\partial \nu_y} g(y,T-t) d\sigma(y) dt, \tag{2.2}$$

where $\partial/\partial\nu_y$ denotes the normal derivative at $y \in \partial\Omega$. In identity (2.2), the dependence of the time-reversal functional $\mathcal{I}_1$ on the boundary data g is explicitly shown. Moreover, since

$$g(y,s) = \int_\Omega \frac{\partial \Gamma}{\partial t}(z,y,0,s) f(z)\, dz \bigg|_{y \in \partial\Omega},$$

it follows that

$$\mathcal{I}_1(x) = \int_\Omega f(z) \int_0^T \int_{\partial\Omega} \frac{\partial G(x,y,T,t)}{\partial \nu_y} \frac{\partial \Gamma}{\partial t}(z,y,0,T-t) d\sigma(y) dt\, dz.$$

2.2. A Modified Time-Reversal Imaging Technique. In this section, we present a modified approach to the time-reversal concept using "free boundary conditions". Introduce a function v_s as the solution to the wave problem

$$\begin{cases} \dfrac{\partial^2 v_s}{\partial t^2}(x,t) - \Delta v_s(x,t) = \dfrac{d\delta_s}{dt}(t) g(x,T-s) \delta_{\partial\Omega}(x), \quad (x,t) \in \mathbb{R}^d \times \mathbb{R}, \\ \\ v_s(x,t) = 0, \quad \partial_t v_s(x,t) = 0, \qquad\qquad x \in \mathbb{R}^d, t \ll s. \end{cases}$$

Here, $\delta_{\partial\Omega}$ is the surface Dirac measure on $\partial\Omega$ and g is the measured data.

We define a modified time-reversal imaging functional by

$$\mathcal{I}_2(x) = \int_0^T v_s(x,T) ds, \quad x \in \Omega.$$

Note that

$$v_s(x,t) = \int_{\partial\Omega} \frac{\partial \Gamma}{\partial t}(x,y,s,t) g(y,T-s)\, d\sigma(y).$$

Consequently, the functional $\mathcal{I}_2$ can be expressed in terms of the free-space Green function Γ as follows

$$\mathcal{I}_2(x) = \int_0^T \int_{\partial\Omega} \frac{\partial \Gamma}{\partial t}(x,y,s,T) g(y,T-s) d\sigma(y) ds, \quad x \in \Omega.$$

Note that $\mathcal{I}_2$ is not exactly equivalent to $\mathcal{I}_1$ but is an approximation. Indeed, with

$$g_\omega(y) = \mathcal{F}[g](y,\omega) = -i\omega \int_\Omega \Gamma_\omega(z,y) f(z)\, dz,$$

Parseval's relation gives

$$\begin{aligned}\mathcal{I}_2(x) &= \int_0^T \int_{\partial\Omega} \frac{\partial\Gamma}{\partial t}(x,y,s,T) g(y,T-s) d\sigma(y) ds \\ &= -\frac{1}{2\pi}\int_{\mathbb{R}}\int_{\partial\Omega} i\omega \Gamma_\omega(x,y)\overline{g}_\omega(y) d\sigma(y) d\omega, \\ &= \frac{1}{2\pi}\int_{\mathbb{R}^d} f(z) \int_{\mathbb{R}}\int_{\partial\Omega} \omega^2 \Gamma_\omega(x,y)\overline{\Gamma}_\omega(z,y) d\sigma(y) d\omega dz\end{aligned}$$

Using the Helmholtz-Kirchhoff identity [**1**]

$$\int_{\partial\Omega} \Gamma_\omega(x,y)\overline{\Gamma}_\omega(z,y) d\sigma(y) \simeq \frac{1}{\omega} Im\left\{\Gamma_\omega(x,z)\right\}$$

which is valid when Ω is a sphere with a large radius in $\mathbb{R}^d$, we find

$$\mathcal{I}_2(x) \simeq \frac{1}{2\pi}\int_{\mathbb{R}^d} f(z) \int_{\mathbb{R}} \omega Im\left\{\Gamma_\omega(x,z)\right\} d\omega dz.$$

Using the identity

$$\frac{1}{2\pi}\int_{\mathbb{R}} \omega Im\left\{\Gamma_\omega(x,z)\right\} d\omega = \delta_z,$$

which follows from the fact that $\partial\Gamma/\partial t(x,z,0,0) = \delta_z$, we finally find that

$$\mathcal{I}_2(x) \simeq f(x).$$

REMARK 2.1. *Our interest in this new time-reversal imaging functional is due to its usefulness for viscous media. Moreover, numerical reconstructions of sources using $\mathcal{I}_1$ or $\mathcal{I}_2$ are quite similar; see the numerical illustrations in Figure 1. In fact, formally, if we let $G_\omega = \mathcal{F}[G]$, then*

$$\mathcal{I}_1(x) = -\frac{i}{2\pi}\int_\Omega f(z) \int_{\mathbb{R}} \omega \int_{\partial\Omega} \frac{\partial G_\omega}{\partial \nu_y}(x,y)\overline{\Gamma_\omega}(z,y) d\sigma(y)\, dz\, d\omega.$$

But by integrating by parts over Ω and recalling that G_ω is real-valued, we have

$$Im \int_{\partial\Omega} \frac{\partial G_\omega}{\partial \nu_y}(x,y)\overline{\Gamma_\omega}(z,y) d\sigma(y) = Im\left\{\Gamma_\omega(x,z)\right\},$$

and therefore,

$$\mathcal{I}_1(x) = f(x),$$

which yields

$$\mathcal{I}_2(x) \simeq \mathcal{I}_1(x).$$

REMARK 2.2. *Note also that the operator $\mathcal{T} : f \to g$ can be expressed in the form*

$$\mathcal{T}(f)(y,t) = g(y,t) = -\int_{\mathbb{R}^d} \frac{\partial\Gamma}{\partial t}(x,y,0,t) f(x) dx, \quad (y,t) \in \partial\Omega \times [0,T].$$

Then its adjoint $\mathcal{T}^*$ satisfies

$$\mathcal{T}^*(g)(x) = \int_0^T \int_{\partial\Omega} \frac{\partial\Gamma}{\partial t}(x,y,t,T) g(y,T-t) d\sigma(y) dt,$$

which is clearly identified to be the time-reversal functional $\mathcal{I}_2$.

3. Time-Reversal Algorithm for Attenuating Acoustic Media

In this section, we present and analyze the concept of time reversal in attenuating acoustic media. We consider the thermo-viscous wave model to incorporate viscosity effect in wave propagation. Let p_a be the solution of the problem

$$\begin{cases} \dfrac{\partial^2 p_a}{\partial t^2}(x,t) - \Delta p_a(x,t) - a\dfrac{\partial}{\partial t}\Delta p_a(x,t) = \dfrac{d\delta_0}{dt} f(x), \quad (x,t) \in \mathbb{R}^d \times \mathbb{R}, \\ \\ p_a(x,t) = 0 = \dfrac{\partial p_a}{\partial t}(x,t), \qquad\qquad t \ll 0, \end{cases}$$

and let $g_a(y,t) = p_a(y,t), (y,t) \in \partial\Omega \times [0,+\infty[$. Again, it is easy to see that g_a is smooth. The problem is to reconstruct the source f from g_a. The strategy of time-reversal is to consider the functional

$$\mathcal{I}_{2,a}(x) = \int_0^T v_{s,a}(x,T)ds, \quad x \in \Omega,$$

where $v_{s,a}$ should now be the solution of the time-reversed attenuated wave equation

$$\begin{cases} \dfrac{\partial^2 v_{s,a}}{\partial t^2}(x,t) - \Delta v_{s,a}(x,t) + a\dfrac{\partial}{\partial t}\Delta v_{s,a}(x,t) = \dfrac{d\delta_s}{dt}\left(g_a(x,T-s)\delta_{\partial\Omega}\right), \quad (x,t) \in \mathbb{R}^d \times \mathbb{R}, \\ \\ v_{s,a}(x,t) = 0 = \dfrac{\partial}{\partial t} v_{s,a}(x,t), \qquad\qquad x \in \mathbb{R}^d, t \ll s. \end{cases}$$

Unfortunately, this problem is ill-posed. Rigorously, we need to regularize the time-reversed attenuated wave equation, for instance by truncating the high frequencies in time or in space.

Introduce the free space fundamental solution $\tilde{\Gamma}_{a,\omega}$ of the Helmholtz equation

$$\omega^2 \widetilde{\Gamma}_{a,\omega}(x,y) + (1 + ia\omega)\,\Delta\widetilde{\Gamma}_{a,\omega}(x,y) = -\delta_x \quad \text{in } \mathbb{R}^d.$$

We have

$$v_{s,a}(x,t) = -\frac{1}{2\pi}\int_{\mathbb{R}} \left\{ \int_{\partial\Omega} i\omega \widetilde{\Gamma}_{a,\omega}(x,y) g_a(y,T-s)d\sigma(y) \right\} \exp(-i\omega(t-s))d\omega,$$

and we can define an approximation $v_{s,a,\rho}$ of the function $v_{s,a}$ as follows

$$v_{s,a,\rho}(x,t) = -\frac{1}{2\pi}\int_{|\omega|\le\rho} \left\{ \int_{\partial\Omega} i\omega \widetilde{\Gamma}_{a,\omega}(x,y) g_a(y,T-s)d\sigma(y) \right\} \exp(-i\omega(t-s))d\omega,$$

where ρ is a regularization parameter. The regularized time-reversal imaging functional defined by

$$\mathcal{I}_{2,a,\rho}(x) = \int_0^T v_{s,a,\rho}(x,T)ds \tag{3.1}$$

is then given by

$$\mathcal{I}_{2,a,\rho}(x) = \int_{\partial\Omega}\int_0^T \frac{\partial}{\partial t}\widetilde{\Gamma}_{a,\rho}(x,y,s,T) g_a(y,T-s)d\sigma(y)ds,$$

where

$$\widetilde{\Gamma}_{a,\rho}(x,y,s,t) = \frac{1}{2\pi}\int_{|\omega|\le\rho} \widetilde{\Gamma}_{a,\omega}(x,y)\exp(-i\omega(t-s))d\omega.$$

REMARK 3.1. *Let $\mathcal{S}'$ be the space of tempered distributions, i.e., the dual of the Schwartz space $\mathcal{S}$ of rapidly decreasing functions (see for instance* [**18**]*). The function $v_{s,a,\rho}(x,t)$ can be identified as the solution of the following wave equation:*

$$\frac{\partial^2 v_{s,a,\rho}}{\partial t^2}(x,t) - \Delta v_{s,a,\rho}(x,t) + a\frac{\partial}{\partial t}\Delta v_{s,a,\rho}(x,t) = S_\rho\left[\frac{d\delta_s}{dt}\right](g_a(x,T-s)\delta_{\partial\Omega}),$$

where S_ρ is the operator defined on the space $\mathcal{S}'$ by

$$S_\rho[\psi](t) = \frac{1}{2\pi}\int_{|\omega|\leq\rho}\exp(-i\omega t)\mathcal{F}[\psi](\omega)d\omega.$$

3.1. Analysis of Regularized Time-Reversal Functional. Recall that $p_a(x,t)$ and $p(x,t)$ are respectively solutions of the wave equations

$$\frac{\partial^2 p_a}{\partial t^2}(x,t) - \Delta p_a(x,t) - a\frac{\partial}{\partial t}\Delta p_a(x,t) = \frac{d\delta_0}{dt}f(x), \quad \text{and} \quad \frac{\partial^2 p}{\partial t^2}(x,t) - \Delta p(x,t) = \frac{d\delta_0}{dt}f(x),$$

and the functions $p_{a,\omega}(x) = \mathcal{F}[p_a](x,\omega)$ and $p_\omega(x) = \mathcal{F}[p](x,\omega)$ are solutions of the Helmholtz equations

$$\left(\kappa(\omega)^2 + \Delta\right)p_{a,\omega}(x) = i\frac{\kappa(\omega)^2}{\omega}f(x), \quad \text{and} \quad \left(\omega^2+\Delta\right)p_\omega(x) = i\omega f(x),$$

respectively, where $\kappa(\omega) = \dfrac{\omega}{\sqrt{1-ia\omega}}$. It can be seen that

$$p_{\omega,a}(x) = \frac{\kappa(\omega)}{\omega}p_{\kappa(\omega)}(x), \quad \text{or} \quad p_a(x,t) = \mathcal{L}_a[p(x,.)](t),$$

where

$$\mathcal{L}_a[\phi](t) = \frac{1}{2\pi}\int_{\mathbb{R}}\frac{\kappa(\omega)}{\omega}\left\{\int_{\mathbb{R}}\phi(s)\exp\{i\kappa(\omega)s\}ds\right\}\exp\{-i\omega t\}d\omega.$$

The following result holds.

PROPOSITION 3.2. *Let $\phi(t)\in\mathcal{S}([0,\infty[)$ (where $\mathcal{S}$ is the Schwartz space). Then,*

$$\mathcal{L}_a[\phi](t) = \phi(t) + \frac{a}{2}\left(t\phi'\right)'(t) + o(a).$$

PROOF. Formally, it follows that

$$\begin{aligned}\mathcal{L}_a[\phi](t) &= \frac{1}{2\pi}\int_{\mathbb{R}}[1+ia/2\omega]\left\{\int_0^\infty[1-\omega^2 a/2s]\phi(s)\exp\{i\omega s\}ds\right\}\exp\{-i\omega t\}d\omega + o(a)\\ &= \phi(t) + \frac{a}{2}\left(-\phi'(t) + (t\phi)''(t)\right) + o(a) = \phi(t) + \frac{a}{2}(t\phi')'(t) + o(a).\end{aligned}$$

This result can be rigorously justified using the stationary phase theorem [**5**]. □

Similarly, introduce the operator $\widetilde{\mathcal{L}}_{a,\rho}$ defined by

$$\widetilde{\mathcal{L}}_{a,\rho}[\phi](t) = \frac{1}{2\pi}\int_0^\infty\phi(s)\left\{\int_{|\omega|\leq\rho}\frac{\widetilde{\kappa}(\omega)}{\omega}\exp\{i\widetilde{\kappa}(\omega)s\}\exp\{-i\omega t\}d\omega\right\}ds,$$

where $\widetilde{\kappa}(\omega) = \dfrac{\omega}{\sqrt{1+ia\omega}}$. By definition, we have

$$\frac{\partial\widetilde{\Gamma}_{a,\rho}}{\partial t} = \widetilde{\mathcal{L}}_{a,\rho}\left[\frac{\partial\Gamma}{\partial t}\right].$$

Moreover, the adjoint operator of $\widetilde{\mathcal{L}}_{a,\rho}$ reads

$$\widetilde{\mathcal{L}}^*_{a,\rho}[\phi](t) = \frac{1}{2\pi}\int_{|\omega|\leq\rho} \frac{\widetilde{\kappa}(\omega)}{\omega}\exp\{i\widetilde{\kappa}(\omega)t\}\left\{\int_0^\infty \phi(s)\exp\{-i\omega s\}ds\right\}d\omega.$$

PROPOSITION 3.3. *Let $\phi(t)\in\mathcal{D}([0,\infty[)$, where $\mathcal{D}([0,\infty[)$ is the space of $\mathcal{C}^\infty$-functions of compact support on $[0,\infty[$. Then for all ρ,*

$$\widetilde{\mathcal{L}}^*_{a,\rho}[\phi](t) = S_\rho[\phi](t) - \frac{a}{2}S_\rho[(t\phi')'] + o(a) \quad as \quad a\to 0.$$

PROOF. Note that, as $\phi(t)\in\mathcal{D}([0,\infty[)$, the support of $\phi\subset[0,T_{\max}]$,

$$\begin{aligned}
\widetilde{\mathcal{L}}^*_{a,\rho}[\phi](t) &= \frac{1}{2\pi}\int_{|\omega|\leq\rho} \frac{\widetilde{\kappa}(\omega)}{\omega}\exp\{i\widetilde{\kappa}(\omega)t\}\left\{\int_0^{T_{\max}} \phi(s)\exp\{-i\omega s\}ds\right\}d\omega \\
&= \frac{1}{2\pi}\int_{|\omega|\leq\rho}\int_0^{T_{\max}} \left[1-ia/2\omega\right]\left[1+\omega^2 a/2t\right]\phi(s)\exp\{-i\omega(s-t)\}dsd\omega + o(a) \\
&= S_\rho[\phi(t)] - \frac{a}{2}S_\rho\left[(t\phi')'\right](t) + o(a).
\end{aligned}$$

□

As an immediate consequence of Propositions 3.2 and 3.3, the following result holds.

PROPOSITION 3.4. *Let $\phi(t)\in\mathcal{D}([0,\infty[)$, then*

$$\widetilde{\mathcal{L}}^*_{a,\rho}\mathcal{L}_a[\phi](t) = S_\rho[\phi](t) + o(a) \quad as \quad a\to 0.$$

We also have the following proposition which shows that using the adjoint of the attenuated wave operator instead of the ideal one is a first order correction of the attenuation effect.

PROPOSITION 3.5. *The regularized time-reversal imaging functional defined by (3.1) satisfies*

$$\mathcal{I}_{2,a,\rho}(x) = -\int_{\partial\Omega}\int_0^T \frac{\partial\Gamma}{\partial t}(x,y,T-s,T)S_\rho[g(y,\cdot)](s)d\sigma(y)ds + o(a),$$

for a small enough.

PROOF. The integral $\mathcal{I}_{2,a,\rho}$ can be rewritten in the form

$$\mathcal{I}_{2,a,\rho}(x) = -\int_{\partial\Omega}\int_0^T \frac{\partial\Gamma}{\partial t}(x,y,T-s,T)\widetilde{\mathcal{L}}^*_{a,\rho}[g_a(y,\cdot)](s)d\sigma(y)ds.$$

Recall as well that $g_a = \mathcal{L}_a[g]$, so that

$$\begin{aligned}
\mathcal{I}_{2,a,\rho}(x) &= -\int_{\partial\Omega}\int_0^T \frac{\partial\Gamma}{\partial t}(x,y,T-s,T)\widetilde{\mathcal{L}}^*_{a,\rho}\mathcal{L}_a[g(y,\cdot)](s)d\sigma(y)ds \\
&= -\int_{\partial\Omega}\int_0^T \frac{\partial\Gamma}{\partial t}(x,y,T-s,T)S_\rho[g(y,\cdot)](s)d\sigma(y)ds + o(a),
\end{aligned}$$

by using Proposition 3.4. □

Finally, observe that the function $\delta_\rho(z)$ defined by

$$\delta_{\rho,x}(z) = \frac{1}{2\pi}\int_{|\omega|\leq\rho} \omega Im\left\{\Gamma_\omega(x,z)\right\} d\omega,$$

is an approximation of the Dirac delta distribution, i.e., $\delta_{\rho,x} \to \delta_x$ as $\rho \to +\infty$. This implies that

$$\begin{aligned} -\int_{\partial\Omega}\int_0^T \frac{\partial}{\partial t}\Gamma(x,y,T-s,T)S_\rho[g(y,\cdot)](s)d\sigma(y)ds \quad &\simeq \quad \delta_{\rho,x} * f \\ &\overset{\rho\to+\infty}{\longrightarrow} \quad f(x), \end{aligned}$$

when x is far away from the boundary $\partial\Omega$.

4. A higher-order reconstruction alternative

In the previous section, we have shown that the time reversal method using the adjoint of attenuated wave operator can be justified as a first order correction of attenuation effect. The algorithm $\mathcal{I}_{2,a,\rho}$ can be seen as a classical time reversal method applied to "preprocessed" data $\widetilde{\mathcal{L}}^*_{a,\rho} g_a$. Moreover, Proposition 3.4 indicates that the operator $\widetilde{\mathcal{L}}^*_{a,\rho}$ is an order one approximation of the inverse of attenuation operator $\mathcal{L}_a$. A higher order correction of attenuation effect can be given using a preprocessed data $\mathcal{L}^{-1}_{a,k} g_a$ instead of using time reversal method with adjoint of attenuated wave operator. Here, the filter $\mathcal{L}^{-1}_{a,k}$ can be defined as an order k approximation of the inverse of operator $\mathcal{L}_a$.

As in our previous work [**5**], the idea is to use an approximation of operator $\mathcal{L}_a$ obtained by a classical argument of stationary phase theorem. More precisely, in the simplified case where $\kappa(\omega) \simeq \omega + i\frac{a}{2}\omega^2$, we have from [**5**] that

$$\mathcal{L}_a[\phi](t) = \sum_{m=0}^{k} \frac{a^m}{m!\, 2^m}\left(t^m\phi'\right)^{(2m-1)}(t) + o(a^k).$$

An approximation of order k of the inverse of operator $\mathcal{L}_a$ can then be given as

$$\mathcal{L}^{-1}_{a,k}\phi = \sum_{m=0}^{k} a^m \phi_{k,m}(t),$$

where $\phi_{k,m}$ is recursively defined by

$$\begin{cases} \phi_{k,0} &= \phi, \\ \phi_{k,m} &= -\displaystyle\sum_{l=1}^{m} \mathcal{D}_l[\phi_{k,m-l}], \end{cases} \quad \text{and} \quad \mathcal{D}_m\phi(t) = \frac{1}{m!\, 2^m}\left(t^m\phi'\right)^{(2m-1)}(t).$$

Thus, a higher-order reconstruction alternative can finally be described in two steps:

Step 1: Preprocess the measured data g_a using the filter $\mathcal{L}^{-1}_{a,k}$;
Step 2: Use the classical time-reversal functional $\mathcal{I}_1$ or $\mathcal{I}_2$ for the reconstruction of the source f.

5. Numerical Illustrations

5.1. Description of the Algorithm. All the wave equations are solved in the box $[-L/2, L/2]^2$ with periodic boundary conditions, where L is supposed to be sufficiently large to prevent any reflection on the boundary. Numerical integrations of each equation are then performed exactly in the Fourier space.

As the solution $v_{s,a,\rho}(x,t)$ is very difficult to obtain numerically, we regularize the problem by truncating high-frequency components in space. This can be seen as an approximation $\widetilde{v}_{s,a,\rho}$ of $v_{s,a,\rho}$, defined as the solution of

$$\frac{\partial^2 \widetilde{v}_{s,a,\rho}}{\partial t^2}(x,t) - \Delta \widetilde{v}_{s,a,\rho}(x,t) + a\frac{\partial}{\partial t}\Delta \widetilde{v}_{s,a,\rho}(x,t) = \frac{d\delta_0}{dt}\chi_\rho\left[(g_a(y,T-s)\delta_{\partial\Omega})\right],$$

where the operator χ_ρ is given by

$$\chi_\rho\left[f\right](x) = \frac{1}{L^2}\sum_{|j|\leq\rho}\int_{[-L/2,L/2]^2} f(z)\exp\left(i\frac{2\pi}{L}(z-x)\cdot j\right)dz.$$

The numerical approximation of $p_a(x,t)$ is obtained by using its spatial Fourier decomposition. Indeed, recall that $p_a(x,t)$ is the solution of wave equation

$$\frac{\partial^2 p_a}{\partial t^2}(x,t) - \Delta p_a(x,t) - a\frac{\partial}{\partial t}\Delta p_a(x,t) = \frac{d\delta_0}{dt}f(x).$$

Therefore, when

$$f(x) = \sum_{j\in\mathbb{Z}^2} f_j \exp\left(-i\frac{2\pi}{L}j\cdot x\right),$$

the function $p_a(x,t)$ can be expanded as

$$p_a(x,t) = \sum_{j\in\mathbb{Z}^2} p_j(t)\exp\left(-i\frac{2\pi}{L}j\cdot x\right),$$

with

$$p_j(t) = \exp\left(-\frac{a}{2}\left(\frac{2\pi}{L}\right)^2|j|^2 t\right)\cos\left(t\sqrt{\left(\frac{2\pi}{L}\right)^2|j|^2 - \frac{a^2}{4}\left(\frac{2\pi}{L}\right)^4|j|^4}\right)f_j.$$

The function $\widetilde{v}_{s,a,\rho}$ can similarly be approximated numerically.

5.2. Experiments. In the sequel, for numerical illustrations Ω is defined in polar coordinate by

$$\Omega = \{(r,\theta)\in[0,\infty[\times[0,2\pi[\ ;\ r\leq 0.95 + 0.05\cos(8\theta)\},$$

and its boundary is discretized by 1024 sensors. The solutions p and $\widetilde{v}_{s,a,\rho}$ are also calculated over $(x,t)\in[-L/2,L/2]^2\times[0,T]$ with $L=4$ and $T=2$, and we used a step of discretization given by $dt = T/2^{10}$ and $dx = L/2^9$.

Figure 1 presents a comparison between the two time reversal imaging functionals $\mathcal{I}_1$ and $\mathcal{I}_2$ for non attenuating acoustic media. One can observe that the two reconstructions are almost identical.

Figure 2 shows some reconstructions using $\mathcal{I}_2$ for an attenuating medium. As expected, the two images obtained respectively with an attenuation coefficient $a = 0.0005$ and $a = 0.001$ appear to be blurred.

Figure 3 presents some reconstructions using $\mathcal{I}_{2,a,\rho}$ for an attenuating medium. The images corresponding to $\mathcal{I}_{2,a,\rho}$ are computed for different values of ρ. It appears that $\mathcal{I}_{2,a,\rho}$

gives a better reconstruction of f than the functional $\mathcal{I}_2$ provided that the regularization parameter ρ is chosen sufficiently large in order to insure the stability of the algorithm.

Figure 4 presents some reconstructions obtained by preprocessing the data with the filter $\mathcal{L}_{a,k}^{-1}$ followed by the time reversal using the imaging functional $\mathcal{I}_2$ in an attenuating medium. This approach is tested by varying the approximation order k. It clearly provides a better reconstruction of f than by using the functional $\mathcal{I}_2$. Moreover, this approach has no instability issues, at least in the numerical simulations presented here.

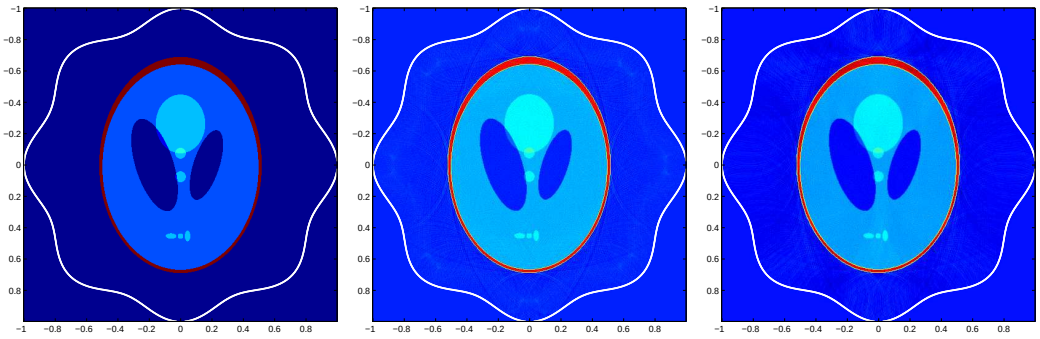

FIGURE 1. Comparison between $\mathcal{I}_1$ and $\mathcal{I}_2$ without attenuation $a = 0$. Left: source $f(x)$; Middle: reconstruction using $\mathcal{I}_1$; Right: reconstruction using $\mathcal{I}_2$.

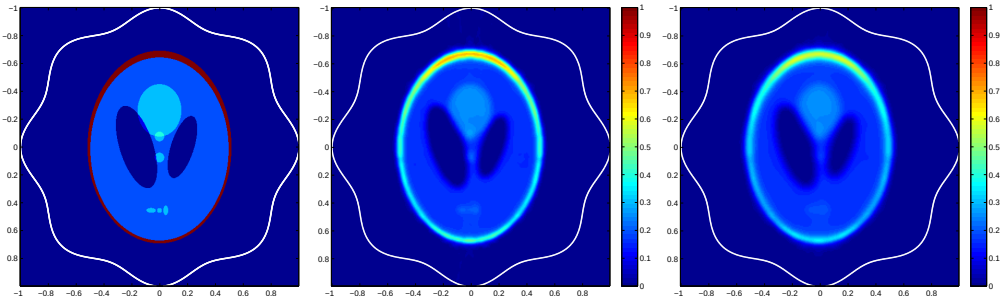

FIGURE 2. Reconstruction using $\mathcal{I}_2$ from attenuated data g_a. Left: source $f(x)$; Middle: reconstruction using $\mathcal{I}_2$ with $a = 0.0005$; Right: reconstruction using $\mathcal{I}_2$ with $a = 0.001$.

6. Discussion and Conclusion

In this work, the attenuation coefficient is assumed to be homogeneous and known a priori. However, in practical situations, this is not the case and an estimation of attenuation coefficient is necessary. An estimation can be done easily if the source f and the data g_a are known simultaneously. Indeed, in this situation, the ideal data g can be recovered from f and a can be estimated as the minimizer of the discrepancy functional J given by

$$J(a) = \left\{ \int_{\partial\Omega} \int_0^T \left| g_a(y,t) - \mathcal{L}_a g(y,t) \right|^2 d\sigma(y) dt \right\}.$$

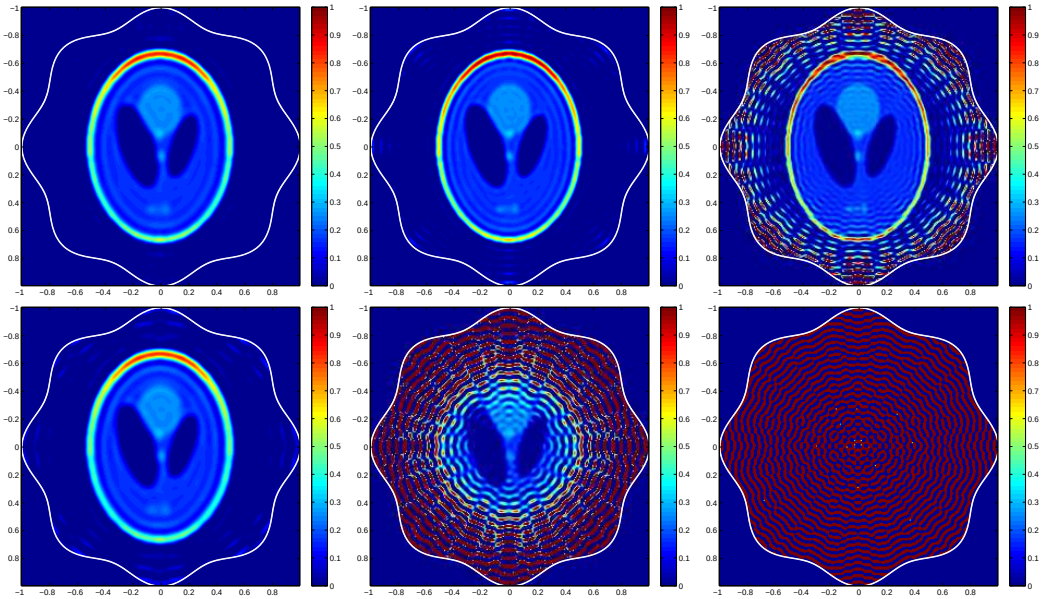

FIGURE 3. Reconstruction using $\mathcal{I}_{2,a,\rho}$ from attenuated data g_a. First line: $a = 0.0005$; Second line: $a = 0.001$; Left: $\rho = 15$; Middle: $\rho = 20$; Right: $\rho = 25$.

In fact, numerical tests using Newton algorithm for solving this optimization problem are quite successful. Figure 5 shows reconstructions of different values of the attenuation coefficient a when the source term f is respectively the phantom, a Gaussian, or a Dirac mass. It turns out that the lower the attenuation coefficient is, the better is the reconstruction. Moreover, The most reliable coefficient reconstruction corresponds to a Dirac mass.

A more involving scenario is when only the data g_a is known. We tried to recover the attenuation coefficient a and the source f simultaneously as the minimizer (a^*, f^*) of the discrepancy functional

$$J(a, f) = \left\{ \int_{\partial\Omega} \int_0^T \left| g_a(y,t) - \mathcal{L}_a \left[\mathcal{T} f(y,t) \right] \right|^2 d\sigma(y) dt \right\},$$

where $\mathcal{T} : f \mapsto g$. However, this optimization problem seems to have an inherent instability issue. This point will be addressed in a future investigation. Another challenging problem is to extract the Green function of attenuating media by correlating waves excited by random sources that are recorder at two locations [**20**]. It is expected that our results in this paper would lead to an efficient approach for solving this problem.

To conclude, the time reversal technique using adjoint attenuated wave operator has clearly provided better resolution in image reconstruction than the classical one without attenuation consideration. We analyzed this approach and proved that it provides a first order correction of the attenuation effects. Unfortunately, this technique is ill-posed and even if a regularization is used, it appears to be unstable and inefficient when the attenuation coefficient a becomes too large. We, therefore, proposed another approach which consists to apply a filter to the measured data followed by a classical time reversal method. This method

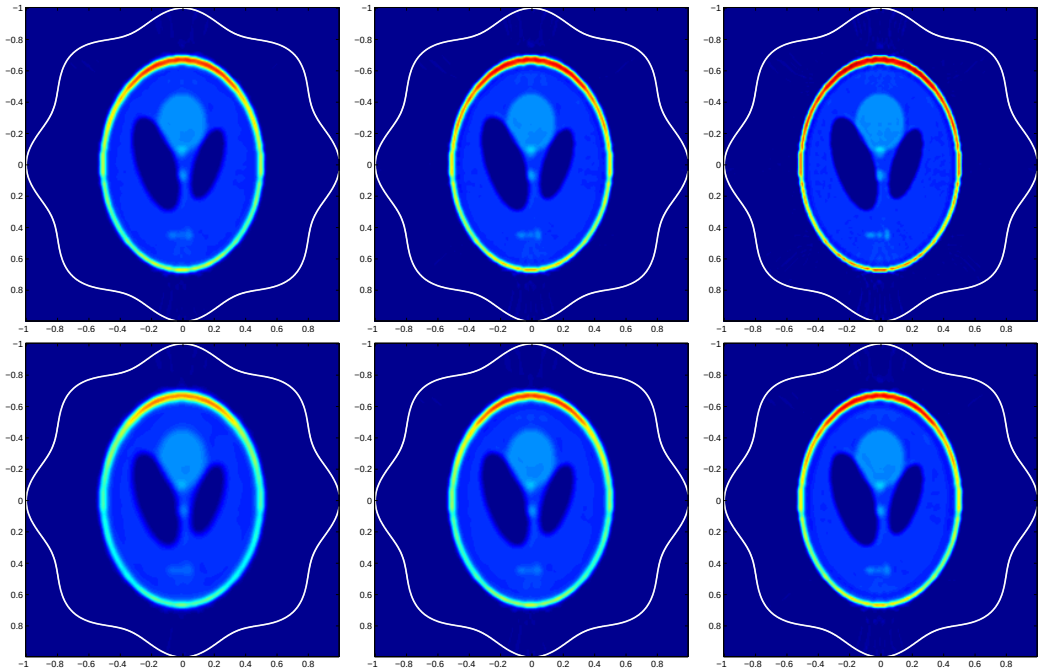

FIGURE 4. Reconstruction by preprocessing the data with the filter $\mathcal{L}_{a,k}^{-1}$ followed by the functional $\mathcal{I}_2$ from attenuated data g_a. First line: $a = 0.0005$; Second line: $a = 0.001$; Left: $k = 1$; Middle: $k = 2$; Right: $k = 4$.

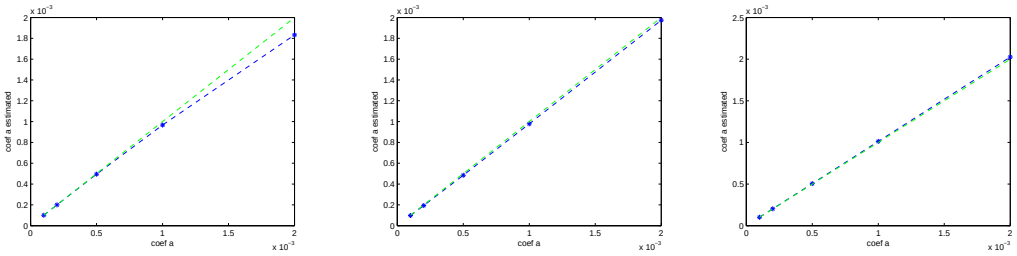

FIGURE 5. Reconstructions of the attenuation coefficient a. Left: the source term f is the phantom; Middle: f is a Gaussian; Right: f is a Dirac mass.

seems to be more stable and accurate as illustrated in our numerical experiments. However, this approach can not be adapted when a depends on spatial variable. In this situation, the attenuated time reversal technique seems to be the best option for attenuation compensation.

References

[1] H. Ammari, *An Introduction to Mathematics of Emerging Biomedical Imaging*, Mathematics & Applications, Vol. 62, Springer-Verlag, Berlin, 2008.

[2] H. Ammari, M. Asch, V. Jugnon, L. Guadarrama Bustos, and H. Kang, *Transient imaging with limited-view data*, SIAM J. Imag. Sci., to appear.

[3] H. Ammari, E. Bossy, V. Jugnon, and H. Kang, Mathematical modelling in photo-acoustic imaging of small absorbers, SIAM Rev., 52 (2010), 677–695.
[4] H. Ammari, E. Bossy, V. Jugnon, and H. Kang, Quantitative photo-acoustic imaging of small absorbers, SIAM J. Appl. Math., to appear.
[5] H. Ammari, E. Bretin, V. Jugnon, and A. Wahab, Photoacoustic imaging for attenuating acoustic media, in *Mathematical Modeling in Biomedical Imaging II*, Lecture Notes in Mathematics, Springer-Verlag, Berlin, to appear.
[6] H. Ammari, Y. Capdeboscq, H. Kang, and A. Kozhemyak, Mathematical models and reconstruction methods in magneto-acoustic imaging, Euro. J. Appl. Math., 20 (2009), 303–317.
[7] H. Ammari, P. Garapon, L. Guadarrama Bustos, and H. Kang, Transient anomaly imaging by the acoustic radiation force, J. Diff. Equat., 249 (2010), 1579–1595.
[8] H. Ammari, L. Guadarrama Bustos, H. Kang, and H. Lee, Transient elasticity imaging and time reversal, Proc. Royal Soc. Edinburgh Sect. A, to appear.
[9] H. Ammari and H. Kang, Expansion Methods, *Handbook of Mathematical Methods in Imaging*, 447–499, Springer-Verlag, New York, 2011.
[10] C. Bardos, A mathematical and deterministic analysis of the time-reversal mirror, in *Inside out: Inverse Problems*, 381–400, MSRI Publ., Vol. 47, 2003.
[11] C. Bardos and M. Fink, Mathematical foundations of the time reversal mirror, Asymptot. Anal., 29 (2002), 157–182.
[12] L. Borcea, G. C. Papanicolaou, C. Tsogka, and J. G. Berrymann, Imaging and time reversal in random media, Inverse Problems, 18 (2002), 1247–1279.
[13] P. Burgholzer, H. Grun, M Haltmeier, R. Nuster, and G. Paltauf, Compensation of acoustic attenuation for high-resolution Photoacoustic imaging with line detectors, Proc. SPIE., 6437 (2007), 643724.
[14] J. de Rosny, G. Lerosey, A. Tourin, and M. Fink, Time reversal of electromagnetic waves, In *Lecture Notes in Comput. Sci. Eng.* , Vol. 59, Springer-Verlag, Berlin, 2007.
[15] M. Fink, Time reversed acoustics, Physics Today 50 (1997), 34.
[16] M. Fink and C. Prada, Acoustic time-reversal mirrors, Inverse Problems, 17 (2001), R1–R38.
[17] J.-P. Fouque, J. Garnier, G. Papanicolaou, and K. Sølna, *Wave Propagation and Time Reversal in Randomly Layered Media*, Springer, New York, 2007.
[18] L. Hörmander, *The Analysis of Linear Partial Differential Operators. I. Distribution Theory and Fourier Analysis*, Classics in Mathematics, Springer-Verlag, Berlin, 2003.
[19] R. Kowar and O. Scherzer, Photoacoustic imaging taking into account attenuation, in *Mathematical Modeling in Biomedical Imaging II*, Lecture Notes in Mathematics, Springer-Verlag, Berlin, to appear.
[20] R. Snieder, Extracting the Green's function of attenuating hetereneous acoustic media from uncorrelated waves, J. Acoust. Soc. Am., 121 (2007), 2637–2643.
[21] M. Tanter and M. Fink, Time reversing waves for biomedical Applications, *Mathematical Modeling in Biomedical Imaging I*, Lecture Notes in Mathematics, Vol. 1983, Springer-Verlag, 2009.
[22] B. E. Treeby, E. Z. Zhang, and B. T. Cox, Photoacoustic tomography in absorbing acoustic media using time reversal, Inverse Problems, 26 (2010), 115003.
[23] Y. Xu and L. V. Wang, Time reversal and its applicaton to tomography with diffraction sources, Physical Review Letters, 92 (2004), 033902.

Department of Mathematics and Applications, École Normale Supérieure, 45 Rue d'Ulm, 75005 Paris, France
E-mail address: habib.ammari@ens.fr

Centre de Mathématiques Appliquées, CNRS UMR 7641, École Polytechnique, 91128 Palaiseau, France
E-mail address: bretin@cmap.polytechnique.fr

Laboratoire de Probabilités et Modèles Aléatoires & Laboratoire Jacques-Louis Lions, Université Paris VII, 75205 Paris Cedex 13, France
E-mail address: garnier@math.jussieu.fr

Centre de Mathématiques Appliquées, CNRS UMR 7641, École Polytechnique, 91128 Palaiseau, France
E-mail address: wahab@cmap.polytechnique.fr